Investigation of Model Micro-scale Reconnecting Plasma Modes

by

Kurt Tummel

Submitted to the Department of Physics in partial fulfillment of the Requirements for the Degree of

BACHELOR OF SCIENCE

at the

MASSACHUSETTS INSTITUTE OF TECHNOLOGY

June, 2008

Thesis Supervisor: Professor Bruno Coppi

Signature of Author ______________________ 5/16/08
Department of Physics

Certified by ______________________
Professor Bruno Coppi
Thesis Supervisor, Department of Physics

____
Chris Crabtree

Accepted by ______________________
Professor David E. Pritchard
Senior Thesis Coordinator, Department of Physics

Abstract

We numerically and analytically investigate the linear complex mode frequencies of model micro-reconnecting plasma modes which have transverse wavelengths of the order of the electron skin depth c/ω_{pe}. This model mode, which can have finite wavelength parallel to the magnetic field, is found in the limit of a straight and uniform magnetic field in the presence of temperature gradients. The theory of the related micro-reconnecting modes has been previously developed in view of explaining the observation of macroscopic instabilities which are not predicted by the drift tearing mode theory [2]. These micro-reconnecting modes are radially localized by magnetic shear and lead to the formation of microscopic magnetic islands. We derive the model dispersion equation, which closely follows the derivation of the micro-reconnecting mode dispersion equation [1], under relevant conditions using the drift kinetic approximation. We also consider the dispersion relation in the fluid limit [1]. We examine the solutions of the resulting dispersion relations and confirm the driving effect of the electron temperature gradient, and the stabilizing effect of a density gradient.

Acknowledgements

I would like to thank Professor Bruno Coppi, for illuminating this project and its complexities throughout my work.

I would also like to thank Chris Crabtree for his guidance and explanation in this project.

Contents

List of Figures

Chapter 1

Introduction

1.1 Background

Currently, approximately 79 percent of the energy used on our planet is generated by burning fossil fuels which release environmentally harmful compounds into our atmosphere [3]. If we were to burn a teaspoon of liquid hydrogen in the presence of oxygen, we would produce water and $40.9kJ$ of energy. If the same teaspoon of hydrogen underwent fusion, we would produce helium, neutrons, and $1.97 \times 10^8 kJ$ of energy. This incredible abundance of energy available through the fusion process, along with its clean byproducts have made fusion energy a very appealing alternative technology. Experts are currently working to design a way to control a fusion reaction and harness the resulting energy.

Present day laboratory plasma experiments relevant to controlled fusion generally have plasma temperatures as high as $15keV$, which would melt any material container we could use. Typically the plasma is contained at low density, and when making contact with the high density material container, it loses large fractions of its energy as it melts the container. An apparent solution to this problem is to use magnetic fields to confine the plasma, as we approach the necessary temperature and density conditions for fusion to occur. One such confinement configuration is the tokamak, an axisymmetric torus with magnetic field lines which wind around the torus with a strong component parallel to the toroidal axis and a weak component which circles the poloidal plane. These field lines result from a toroidal field component which is generated externally by coils, and a poloidal field which is generated by the currents in the plasma.

This magnetic field configuration is able to overcome the loss of plasma confinement due to particle drifts, which arise from the gradients and curvature of the magnetic field and the electric field. However, we still struggle with plasma confinement because of instabilities like those resulting from magnetic reconnection. Magnetic reconnection is a phenomenon in which the magnetic field lines in a plasma magnetic field configuration break apart and reconnect in a way that can facilitate energy and particle transport. Further efforts to design a controlled magnetically confined fusion device rely on a strong theoretical understanding of these magnetic reconnection events, and the relevant plasma modes.

1.2 Motivation

Magnetic reconnection and the associated magnetic island structures have been consistently observed in well confined, high temperature plasmas [4]. Existing models of magnetic reconnection such as the drift-tearing mode which explain such instabilities in lower temperature regimes do not predict instabilities in these conditions. This is due to the stabilizing effect of electron Landau damping in the collisionless case, and to the parallel thermal conductivity in the weakly collisional case. These reconnection events and the associated structures can be explained with micro-reconnecting mode theory. In the theory, the micro-reconnecting modes are radially localized about the reference surface where $k_{\|} \equiv \mathbf{k} \cdot \mathbf{B}/B \simeq 0$. In the presence of magnetic shear, these modes lead to the formation of microscopic magnetic islands with transverse scale length c/ω_{pe}. These islands are created by an electromagnetic instability driven primarily by the electron temperature gradient. The microscopic islands increase the ratio of transverse to longitudinal thermal conductivity considerably over its classical value. It is this increase which alters the stability criterion of the drift tearing modes and permits the meso-scale magnetic reconnection, which is ultimately driven by the current density gradient [2].

We investigate the model micro-reconnecting modes, which are derived without the presence of magnetic shear and with $k_{\|} \neq 0$. Modes of this type may be observed experimentally and this analysis serves as a foundation for further theoretical investigation of the micro-reconnecting modes.

In this thesis we investigate the stability of these model micro-reconnecting modes. In Chapter 2 we detail the relevant derivation of the dispersion equation. Then in Chapter 3 we analyze the solutions of the mode frequencies under various conditions. We make some concluding remarks about our results and future projects in Chapter 4.

Chapter 2

Model Micro-Reconnecting Modes

2.1 Dispersion Relation Derivation

In attempting to understand these model micro-reconnecting plasma modes, we will examine the solutions of the relevant mode dispersion relation under various conditions. We proceed by reproducing the dispersion relation derivation previously obtained by Bruno Coppi [1] for the related micro-reconnecting modes. The contents of this chapter closely follow these notes, though we make simplifying approximations in our derivation which distinguish our resulting mode from the similar micro-reconnecting modes. In the micro-reconnecting mode theory, the magnetic shear is introduced through the equilibrium magnetic field

$$\mathbf{B} = B_0(\mathbf{e}_z + \frac{x}{L_s}\mathbf{e}_y) \tag{2.1}$$

such that x corresponds to the radial distance from some reference rational surface. The y and z coordinates correspond to the angular displacement in the poloidal plane, and along the toroidal axis, respectively. This coordinate system, along with the expected magnetic field lines in the tokamak are shown in Figure 2.1. From the

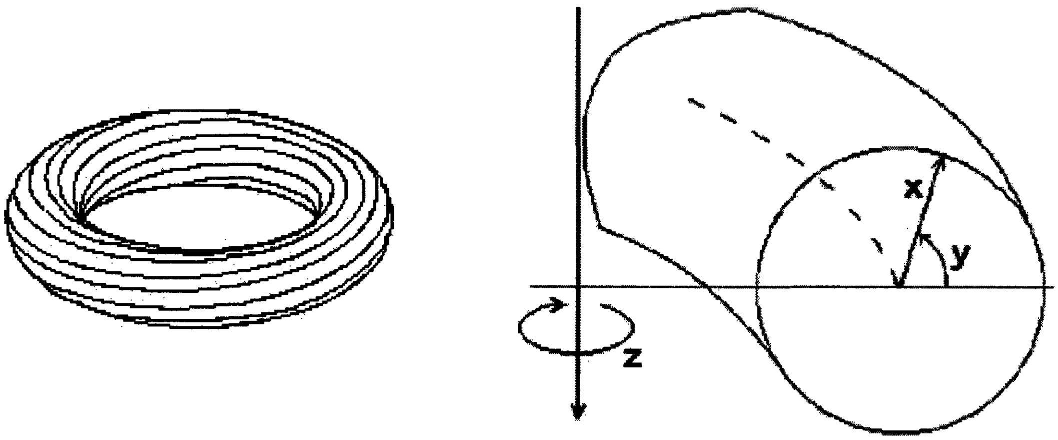

Figure 2.1: The magnetic field lines in the Tokamak configuration are shown on the left. The coordinate system is depicted on the right

MHD equation of motion in equilibrium conditions,

$$\nabla p \simeq \frac{1}{c}\mathbf{J} \times \mathbf{B}.$$

and the relation $\nabla \times \mathbf{B} = \frac{4\pi}{c}\mathbf{J}$, our equilibrium magnetic field given in Eq. (2.1) must be balanced by an equilibrium pressure that depends on x. It also follows that the equilibrium temperature and density are independent of y and z. In the present analysis we neglect magnetic shear by considering $x/L_s \ll 1$ and thus $\mathbf{B} \simeq B_0\mathbf{e}_z$, though we maintain that the equilibrium density and temperature depend on x. To derive the dispersion relation we utilize the drift kinetic approximation which averages out the gyrating motion of the charged particles. We consider the motion of the guiding centers of the particles which can be approximated to first order as the $\mathbf{E} \times \mathbf{B}$

drift velocity

$$\mathbf{v}_{gc} \simeq \frac{c\mathbf{E} \times \mathbf{B}}{B^2}$$

We begin with the linear phase space density equation for electrons which is given as

$$\frac{\partial \hat{f}_e}{\partial t} + \nabla \cdot \{[\frac{\mathbf{B}}{B} v_{\|}]\, \hat{f}_e\} = -\nabla \cdot \{[\frac{\hat{\mathbf{B}}}{B} v_{\|} - \frac{\mathbf{B}\hat{B}}{B^2} v_{\|} + \hat{\mathbf{v}}_{gc}]\, f_e\} + \frac{e}{m_e} \hat{E}_{\|} \tag{2.2}$$

where f_e, $\hat{f}_e$ are the equilibrium and perturbed phase space density respectively, and $\hat{\mathbf{E}}_{\|}$ is the perturbed parallel component of the electric field. We use potentials to represent perturbed electromagnetic fields $\hat{\mathbf{E}} = -\nabla\hat{\Phi} - \frac{1}{c}\frac{\partial}{\partial t}\hat{\mathbf{A}}$, $\hat{\mathbf{B}} = \nabla \times \hat{\mathbf{A}}$. Then the perturbed guiding center velocity is

$$\hat{\mathbf{v}}_{gc} \cong -\frac{c[\nabla\hat{\Phi} + \frac{1}{c}\frac{\partial \hat{\mathbf{A}}}{\partial t}] \times \mathbf{B}}{B^2}$$

We can reduce this equation with the simplifying approximation

$$\hat{\mathbf{A}} \simeq \hat{A}_{\|} \frac{\mathbf{B}}{B} \quad \rightarrow \quad \hat{\mathbf{B}} = \nabla \hat{A}_{\|} \times \frac{\mathbf{B}}{B} + A_{\|} \nabla \times \frac{\mathbf{B}}{B} \simeq \nabla \hat{A}_{\|} \times \frac{\mathbf{B}}{B} \tag{2.3}$$

where the curl of the equilibrium magnetic field unit vector vanishes in our case where the field lines are virtually straight. We have also neglected $\hat{B}_{\|}$ so that we may rewrite the pertubed guiding center velocity as

$$\hat{\mathbf{v}}_{gc} \simeq -\frac{c\nabla\hat{\Phi} \times \mathbf{B}}{B^2}$$

Returning to Eq. (2.2) we see that the guiding center velocity appears as

$$\nabla \cdot \{[\frac{c\nabla\hat{\Phi} \times \mathbf{B}}{B^2}]\, f_e\} = \nabla \cdot \{\frac{c\nabla\hat{\Phi} \times \mathbf{B}}{B^2}\} f_e + \frac{c\nabla\hat{\Phi} \times \mathbf{B}}{B^2} \cdot \nabla f_e \simeq \frac{c}{B}\frac{\partial \hat{\Phi}}{\partial y}\frac{\partial f_e}{\partial x} \tag{2.4}$$

Where the $\hat{\mathbf{E}} \times \mathbf{B}$ motion is approximately incompressible, and we have used the fact that the equilibrium only depends on x. We continue by taking advantage of the fact that $\nabla \cdot \hat{\mathbf{B}} \simeq 0$ and the relations given in Eq. (2.3) to impose the following simplification

$$
\begin{aligned}
-\nabla \cdot \{[\frac{\hat{\mathbf{B}}}{B} v_\| - \frac{\mathbf{B}\hat{B}}{B^2} v_\|]\, f_e\} &\simeq -\nabla \cdot \{[\nabla \hat{A}_\| \times \frac{\mathbf{B}}{B^2} v_\|]\, f_e\} \\
&= -v_\| [\nabla \hat{A}_\| \times \frac{\mathbf{B}}{B}] \cdot \mathbf{e}_x \frac{d}{dx} \frac{f_e}{B} \simeq -\frac{v_\|}{B} \frac{\partial \hat{A}_\|}{\partial y} \frac{\partial f_e}{\partial x}
\end{aligned}
\tag{2.5}
$$

where again we discard the contribution of y and z in the dot product because the equilibrium only depends on x. With Eq. (2.4) and Eq. (2.5) we can rewrite Eq. (2.2)

$$
\frac{\partial \hat{f}_e}{\partial t} + \nabla \cdot \{[\frac{\mathbf{B}}{B} v_\|]\, \hat{f}_e\} = -\frac{v_\|}{B} \frac{\partial \hat{A}_\|}{\partial y} \frac{\partial f_e}{\partial x} + \frac{c}{B} \frac{\partial \hat{\Phi}}{\partial y} \frac{\partial f_e}{\partial x} + \frac{e}{m_e} \hat{E}_\| \tag{2.6}
$$

Now we introduce the following Fourier-Laplace representations.

$$
\hat{f}_e = \tilde{f}_e \, \mathrm{e}^{ik_x x + ik_y y + ik_z z - i\omega t}
$$

$$
\hat{\Phi} = \tilde{\Phi} \, \mathrm{e}^{ik_x x + ik_y y + ik_z z - i\omega t}
$$

$$
\hat{A}_\| = \tilde{A}_\| \, \mathrm{e}^{ik_x x + ik_y y + ik_z z - i\omega t}
$$

where the tilde represents a perturbed quantity. Combining these expressions with Eq. (2.6) we have

$$
(\omega - k_\| v_\|)\tilde{f}_e \simeq \frac{k_y}{B}(v_\| \tilde{A}_\| - c\tilde{\Phi}) \frac{\partial f_e}{\partial x} - \frac{e}{m_e}(k_\| \tilde{\Phi} - \frac{\omega}{c} \tilde{A}_\|) \frac{\partial f_e}{\partial v_\|} \tag{2.7}
$$

where in the present we define $k_\| \equiv \mathbf{k} \cdot \mathbf{B}/B \simeq k_z$. Then we consider an equilibrium Maxwelian distribution,

$$
f_e = n(x) \sqrt{\frac{m_e}{2\pi T_e(x)}} \, \mathrm{e}^{-m_e v_\|^2 / 2T_e(x)}
$$

with which we can further reduce Eq. (2.7)

$$
\begin{aligned}
(\omega - k_\| v_\|)\tilde{f}_e \simeq \frac{k_y}{B}(v_\| \tilde{A}_\| - c\tilde{\Phi})(\frac{1}{n}\frac{dn}{dx} - \frac{1}{2T_e}\frac{dT_e}{dx} + \frac{m_e v_\|^2}{2T_e^2}\frac{dT_e}{dx}[v_\perp^2 + v_\|^2]) f_e \\
+ \frac{e}{m_e}(k_\| \tilde{\Phi} - \frac{\omega}{c} \tilde{A}_\|)(\frac{m_e v_\|}{T_e} f_e)
\end{aligned}
\tag{2.8}
$$

To close the system of equations self consistently we need to find the perturbed electromagnetic fields in terms of the perturbed distribution function. We accomplish this by using the linear phase space density equation to calculate the perturbed parallel current and perturbed charge density. Then we impose the quasineutrality condition and Ampere's law as follows

$$0 \simeq -4\pi e[\hat{n}_i - 2\pi \int v_\perp dv_\perp dv_\parallel \hat{f}_e]$$
$$\nabla^2 \hat{A}_\parallel = -\frac{4\pi e}{c} 2\pi \int v_\perp dv_\perp dv_\parallel v_\parallel \hat{f}_e$$

We take the ion response to be adiabatic ($k_\perp \rho_i > 1$), and we take k_x^2 ,$k_y^2 > k_z^2$ so that these expressions take the form

$$0 \simeq -4\pi e[-\frac{e\tilde{\Phi}}{T_i} n - 2\pi \int v_\perp dv_\perp dv_\parallel \tilde{f}_e] \tag{2.9}$$
$$(-k_x^2 - k_y^2)\tilde{A}_\parallel = -\frac{4\pi e}{c} 2\pi \int v_\perp dv_\perp dv_\parallel v_\parallel \tilde{f}_e \tag{2.10}$$

To take advantage of the quasineutrality condition and Ampere's law we solve Eq. (2.8) for $\tilde{f}_e$ and integrate over $v_\perp$, where we integrate over the same range of $v_\perp$ for Eq. (2.9) and Eq. (2.10). We find that

$$2\pi \int_0^\infty v_\perp dv_\perp \tilde{f}_e = \frac{1}{\omega - k_\parallel v_\parallel}[v_\parallel \tilde{A}_\parallel - c\tilde{\Phi}]\frac{1}{B}\{\frac{1}{n}\frac{dn}{dx} - \frac{1}{2T_e}\frac{dT_e}{dx} + \frac{m_e v_\parallel^2}{2T_e^2}\frac{dT_e}{dx} v_\parallel^2\} nF_e$$
$$+ \frac{1}{\omega - k_\parallel v_\parallel}\frac{e}{m_e}(k_\parallel \tilde{\Phi} - \frac{\omega}{c}\tilde{A}_\parallel)\frac{m_e v_\parallel}{T_e} nF_e$$

Where $F_e \equiv \int_0^\infty v_\perp dv_\perp f_e$. Now to simplify the expression above, we introduce the following diamagnetic frequencies,

$$\omega_{*Te} \equiv \frac{ck_y T_e}{eB}\frac{1}{T_e}\frac{dT_e}{dx} \quad \omega_{*e} \equiv \frac{ck_y T_e}{eB}\frac{1}{n}\frac{dn}{dx}$$

so that

$$2\pi \int_0^\infty v_\perp dv_\perp \tilde{f}_e = -\frac{e}{T_e} nF_e \tilde{\Phi} + \frac{e}{T_e}\frac{\omega_{*e} - \frac{1}{2}\omega_{*Te} + \omega_{*Te} v_\parallel^2 \frac{m_e}{2T_e} - \omega}{\omega - k_\parallel v_\parallel}[\frac{v_\parallel}{c}\tilde{A}_\parallel - \tilde{\Phi}] nF_e$$

Combining this result with Eq. (2.10), we find that

$$[k_x^2 + k_y^2]\tilde{A}_\| = \frac{4\pi e^2}{cT_e} n \int_{-\infty}^{\infty} dv_\| \frac{\omega_{*e} - \frac{1}{2}\omega_{*Te} + \omega_{*Te} v_\|^2 \frac{m_e}{2T_e} - \omega}{\omega - k_\| v_\|} [\frac{v_\|}{c}\tilde{A}_\| - \tilde{\Phi}] v_\| F_e$$

If we introduce the following definitions $d_e^2 \equiv c^2/\omega_{pe}^2$, and $\omega_{pe}^2 \equiv 4\pi n e^2/m_e$, and $v_{te} \equiv \sqrt{2T_e/m_e}$, we can rewrite this equation as

$$[d_e^2 k_x^2 + d_e^2 k_y^2]\tilde{A}_\| = \frac{m_e c}{T_e} \int_{-\infty}^{\infty} dv_\| \frac{\omega_{*e} + \omega_{*Te}(v_\|^2/v_{te}^2 - \frac{1}{2}) - \omega}{\omega - k_\| v_\|} [\frac{v_\|}{c}\tilde{A}_\| - \tilde{\Phi}] v_\| F_e \quad (2.11)$$

Manipulating Eq. (2.9) in the same way we arrive at

$$0 \simeq -[1 + \frac{T_e}{T_i}]\tilde{\Phi} + \int_{-\infty}^{\infty} dv_\| \frac{\omega_{*e} + \omega_{*Te}(v_\|^2/v_{te}^2 - \frac{1}{2}) - \omega}{\omega - k_\| v_\|} [\frac{v_\|}{c}\tilde{A}_\| - \tilde{\Phi}] F_e \quad (2.12)$$

We proceed by introducing Ω_* defined as

$$\Omega_* \equiv \frac{\omega^2}{\sqrt{\pi}} \int_{-\infty}^{\infty} du 2u^2 e^{-u^2} (\frac{\omega_{*e} + \omega_{*Te}(u^2 - 1/2) - \omega}{\omega^2 - k_\|^2 v_{te}^2 u^2})$$

where $u \equiv v_\|/v_{te}$. Then by utilizing the fact that the integral of an odd power of u over $-\infty < u < \infty$ is zero, we can reduce Eq. (2.12) to give a relation between $\tilde{\Phi}$ and $\tilde{A}_\|$

$$\tilde{\Phi} \simeq \frac{v_{te}^2 k_\| \Omega_*/2c\omega^2}{T_e/T_i + \omega_{*e}/\omega + k_\|^2 v_{te}^2 \Omega_*/2\omega^3} \tilde{A}_\|$$

Combining this result with Eq. (2.11) we arrive at the following result

$$(\omega^3[1 + \frac{T_i}{T_e}\frac{\omega_{*e}}{\omega}] + \frac{1}{2}k_\|^2 c_{se}^2 \Omega_*)(d_e^2 k_x^2 + d_e^2 k_y^2)\tilde{A}_\| \simeq \omega^2 \Omega_* \tilde{A}_\| [1 + \frac{T_i}{T_e}\frac{\omega_{*e}}{\omega}] \quad (2.13)$$

where $c_{se} \equiv \sqrt{2T_i/m_e}$. Then by carefully adding zero to the argument of the integral in Ω_*, we can simplify the integrals we need to compute in searching for the solutions of the resulting expression. We find that

$$\Omega_* = \omega_{*Te}(1 + F_0^0) - (\omega - \omega_{*e})(1 + G_0^0)$$

where

$$F_0^0 \equiv \frac{1}{\sqrt{\pi}} \int_{-\infty}^{\infty} du 2u^2 \mathrm{e}^{-u^2} (\frac{(u^2(u^2-1/2))}{\Lambda^2 - u^2})$$
$$G_0^0 \equiv \frac{1}{\sqrt{\pi}} \int_{-\infty}^{\infty} du 2u^2 \mathrm{e}^{-u^2} (\frac{u^2}{\Lambda^2 - u^2})$$

Rearranging the terms we find [1]

$$\frac{\bar{k}^2}{2+2\bar{k}^2}[\Lambda\tau + (\Lambda\tau - \frac{2\Lambda^3}{\bar{k}^2})G_0^0] - \alpha\frac{\bar{k}^2}{2+2\bar{k}^2}[\tau - \frac{2\Lambda^2}{\bar{k}^2}(1-\tau) - \frac{2\Lambda}{\bar{k}^2}\alpha\tau](1+G_0^0)$$
$$\simeq \Lambda^3 + D[1 - \frac{2\Lambda^2}{\bar{k}^2\tau}](1+F_0^0) - \alpha D\frac{2\Lambda}{\bar{k}^2}(1+F_0^0) + \alpha\Lambda^2\tau\frac{\bar{k}^2}{1+\bar{k}^2} \quad (2.14)$$

where

$$D \equiv \frac{\omega_{*Te}}{|k_\parallel|v_{te}}\frac{\bar{k}^2}{2+2\bar{k}^2}, \quad \Lambda \equiv \frac{\omega}{|k_\parallel|v_{te}}, \quad \bar{k}^2 \equiv (k_x^2 + k_y^2)d_e^2, \quad \alpha \equiv \frac{\omega_{*e}}{|k_\parallel|v_{te}}, \quad \tau \equiv \frac{T_i}{T_e}$$

The details of these final steps are outlined in Appendix A.

2.2 Fluid Limit

We also wish to investigate these model micro-reconnecting modes in the fluid limit, where $\omega/k_\parallel v_{te} \gg 1$. In this case we can make the following expansion

$$\frac{\omega^2}{\omega^2 - k_\parallel^2 v_{te}^2 u^2} \sim 1 + \frac{k_\parallel^2 v_{te}^2}{\omega^2}u^2$$

Refering back to our definition of Ω_* we have

$$\Omega_* \sim \frac{1}{\sqrt{\pi}} \int_{-\infty}^{\infty} du\, \mathrm{e}^{-u^2} 2u^2 [\omega_{*e} + \omega_{*Te}(u^2 - 1/2) - \omega](1 + \frac{k_\parallel^2 v_{te}^2}{\omega^2}u^2)$$

In our analysis we introduce the parameter $\epsilon \equiv k_\parallel^2 v_{te}^2/\omega^2 \ll 1$ and we assume the following orderings $\omega_{*e}/\omega_{*Te} \sim \omega/\omega_{*Te} \sim \epsilon$. In these conditions $\Omega_* \simeq \omega_{*Te}$, and from

Eq. (2.13) we find the following result for the model micro-reconnecting modes in the fluid limit.

$$(\omega^3[1+\frac{T_i\,\omega_{*e}}{T_e\,\omega}]+\frac{1}{2}k_\parallel^2c_{se}^2\omega_{*Te})(d_e^2k_x^2+d_e^2k_y^2)\simeq\omega^2\omega_{*Te}[1+\frac{T_i\,\omega_{*e}}{T_e\,\omega}]$$

After rearranging the terms we have

$$\frac{2\omega^3}{k_\parallel^2c_{se}^2\omega_{*Te}}[1+\frac{T_i\,\omega_{*e}}{T_e\,\omega}]+1\simeq\frac{1}{d_e^2k_x^2+d_e^2k_y^2}\frac{2\omega^2}{k_\parallel^2c_{se}^2}[1+\frac{T_i\,\omega_{*e}}{T_e\,\omega}]$$

and introducing the following definitions

$$\bar{\omega}\equiv\omega(\frac{2}{k_\parallel^2c_{se}^2\omega_{*Te}})^{1/3},\quad A\equiv\frac{\omega_{*e}T_i}{T_e}(\frac{2}{k_\parallel^2c_{se}^2\omega_{*Te}})^{1/3},\quad k_0^2=(d_e^2k_x^2+d_e^2k_y^2)(\frac{k_\parallel^2c_{se}^2}{2\omega_{*Te}^2})^{1/3}$$

we arrive at our desired dispersion relation [1]

$$\bar{\omega}^3(1+\frac{A}{\bar{\omega}})+1\simeq\frac{1}{k_0^2}\bar{\omega}^2(1+\frac{A}{\bar{\omega}})\tag{2.15}$$

which is cubic in the complex mode frequency. There are two real parameters, k_0^2 which is related to the temperature gradient, and A which is related to the effect of a density gradient.

Chapter 3

Numerical Analysis and Results

Now we wish to investigate the model micro-reconnecting modes by analyzing the solutions of the dispersion relations derived in Chapter 2.

3.1 The Fluid Limit

We begin by analyzing the solutions of Eq. (2.15), which was derived in the fluid limit.

$$\bar{\omega}^2(\bar{\omega}+A)+1 \simeq \frac{1}{k_0^2}\bar{\omega}(\bar{\omega}+A) \tag{3.1}$$

where we recall

$$\bar{\omega} \equiv \omega(\frac{2}{k_\parallel^2 c_{se}^2 \omega_{*Te}})^{1/3}, \quad A \equiv \frac{\omega_{*e} T_i}{T_e}(\frac{2}{k_\parallel^2 c_{se}^2 \omega_{*Te}})^{1/3}, \quad k_0^2 = (d_e^2 k_x^2 + d_e^2 k_y^2)(\frac{k_\parallel^2 c_{se}^2}{2\omega_{*Te}^2})^{1/3}$$

In producing our solution curves we take A real and hold it constant and find the solutions of $\bar{\omega}$, which corresponds to the scaled micro-reconnecting mode frequency, for various values of k_0. We find that $\bar{\omega}$ is purely real as long as k_0 remains below a critical value k_{crit}. The imaginary part of $\bar{\omega}$ reaches its maximum value as k_0 goes to infinity, but reaches nearly peak value at around $k_0 \simeq 2$ for values of $A \leq 5$. A plot of this is shown in Figure 3.1, along with a plot of $\bar{\omega}$ in the complex plane for $2 > k_0 > k_{crit}$ and several values of A. As expected from a cubic equation, the complex solutions come in pairs, and in addition to unstable roots we find damped modes. It would appear from this figure that as we increase A which can be interpreted as a density gradient parameter, that the mode frequencies diminish. We took $k_0 = 2$ and found $\bar{\omega}$ for A ranging from 0 to 10 as shown in Figure 3.2, and confirmed the suppressing effect of A. We also wish to uncover a relation between A and the associated critical value of k_0 at which the solutions $\bar{\omega}$ become complex. We expect this transition to occur when the first derivative of Eq. (3.1) with respect to $\bar{\omega}$ is zero. Differentiating Eq.(3.1) with respect to $\bar{\omega}$ we have

$$\bar{\omega}^2 = \frac{A}{3k_0^2} + \frac{2\bar{\omega}}{3}(\frac{1}{k_0^2} - A) \tag{3.2}$$

If we define $C_0 \equiv \frac{1}{k_0^2} - A$ and substitute Eq. (3.2) into Eq. (3.1) it becomes first order in $\bar{\omega}$.

$$(\frac{2A}{3k_0^2} + \frac{2}{9}C_0^2)\omega = -\frac{A}{9k_0^2}C_0 + 1 \tag{3.3}$$

Now we use the solution of Eq. (3.2), which we find from the quadratic formula

$$\omega = \frac{1}{3}C_0 + \sqrt{\frac{1}{9}C_0^2 + \frac{A}{3k_0^2}} \tag{3.4}$$

to eliminate $\bar{\omega}$ from Eq. (3.3). We simplify the resulting expression to find the following relation between A and the critical values of k_0

$$4A^3k_0^8 + 27k_0^8 + 6A^2k_0^6 - A^4k_0^4 - 6Ak_0^4 - 2A^3k_0^2 - 4k_0^2 - A^2 = 0 \tag{3.5}$$

We examined Eq. (3.1) numerically to find a plot of critical values of k_0 versus A which agreed with our analytical prediction above as shown in Figure 3.3.

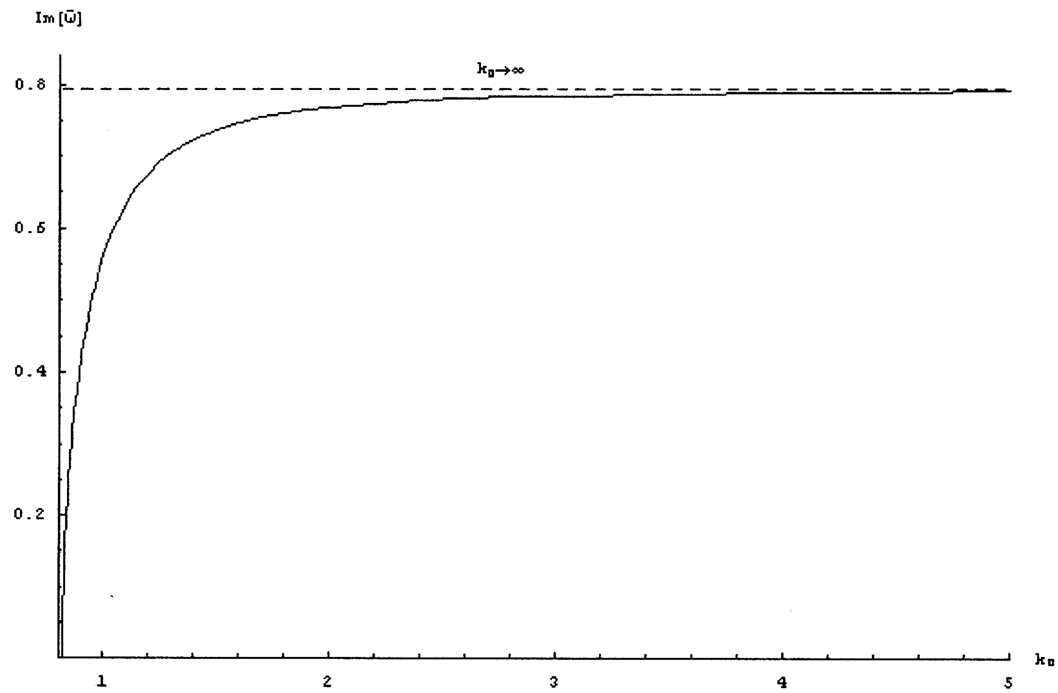

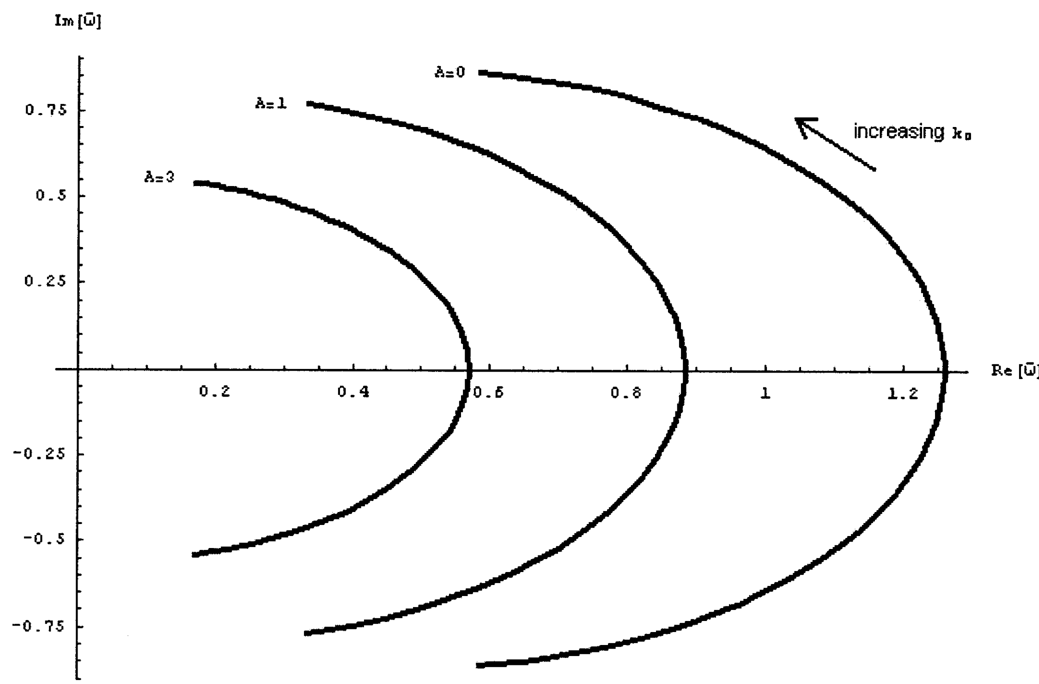

Figure 3.1: Above: $\text{Im}[\bar{\omega}]$ as $k_0 \to \infty$ for $A = 1$, Below: $\bar{\omega}$ in the complex plane for $2 > k_0 > k_{crit}$ and $A = 0, 1, 3$

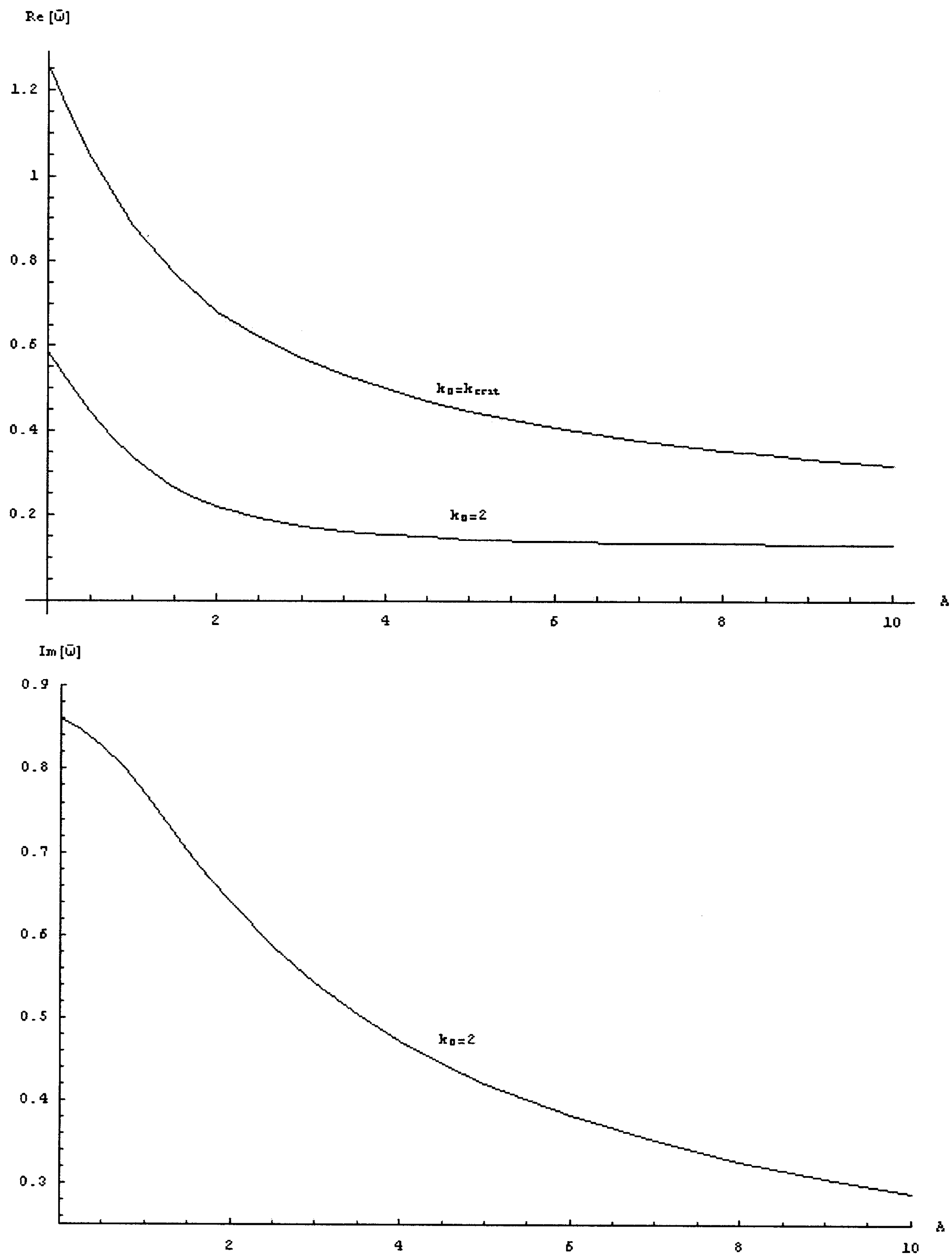

Figure 3.2: Above: Re[$\bar{\omega}$] versus A for $k_0 = k_{crit}$ and $k_0 = 2$, Below: Im[$\bar{\omega}$] versus A for $k_0 = 2$

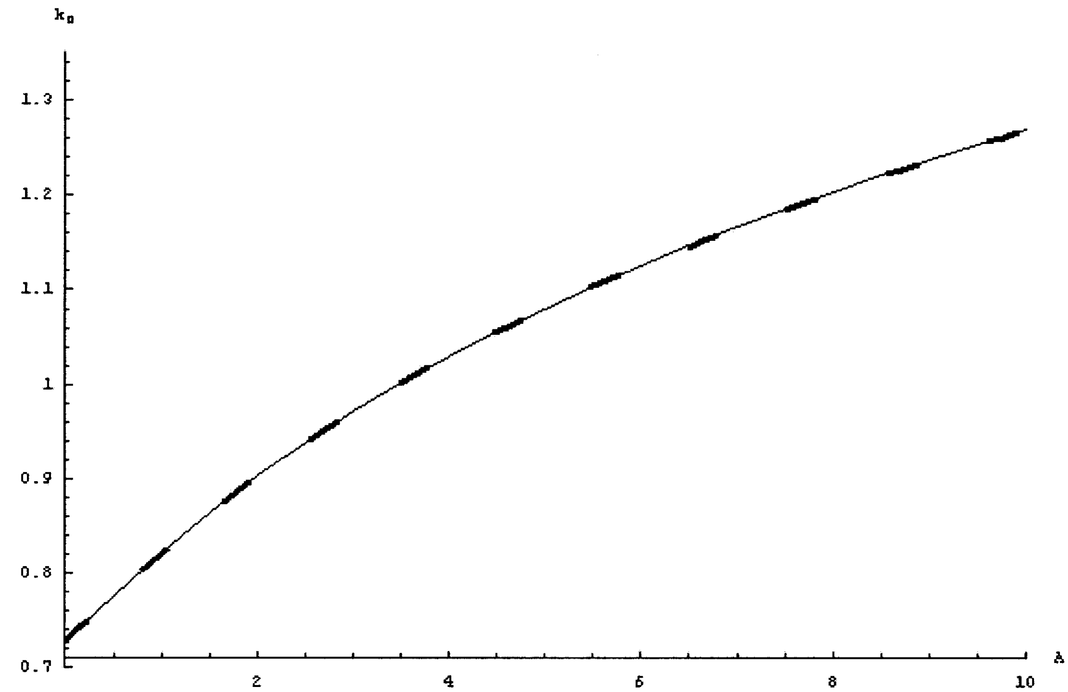

Figure 3.3: The bold dashed line is our analytical prediction given in Eq. (3.5), and the fine line is our numerical confirmation

3.2 The Drift-Kinetic Approximation

Now we will analyze the solutions of our dispersion relation derived with the drift-kinetic approximation given in Eq. (2.14). We begin this analysis by considering the case where $\tau = T_i/T_e = 1$, and $\frac{dT_e}{dx}/\frac{dn}{dx} \gg 1$. In these conditions we may neglect the contribution of the density gradient which appears in the variable α through the frequency ω_{*e}. The resulting equation is

$$\Lambda^3 + D[1 - \frac{2\Lambda^2}{\bar{k}^2}](1 + F_0^0) = \frac{\bar{k}^2}{2 + 2\bar{k}^2}[\Lambda + (\Lambda - \frac{2\Lambda^3}{\bar{k}^2})G_0^0] \tag{3.6}$$

were we recall

$$D \equiv \frac{\omega_{*Te}}{|k_\parallel| v_{te}} \frac{\bar{k}^2}{2 + 2\bar{k}^2}, \quad \Lambda \equiv \frac{\omega}{|k_\parallel| v_{te}}, \quad \bar{k}^2 \equiv d_e^2 k_x^2 + d_e^2 k_y^2$$

and

$$F_0^0 \equiv \frac{1}{\sqrt{\pi}}\int_{-\infty}^{\infty} du 2u^2 e^{-u^2}(\frac{(u^2(u^2-1/2))}{\Lambda^2-u^2})$$
$$G_0^0 \equiv \frac{1}{\sqrt{\pi}}\int_{-\infty}^{\infty} du 2u^2 e^{-u^2}(\frac{u^2}{\Lambda^2-u^2})$$

The solutions to Eq. (3.6) give Λ, which corresponds to the scaled model micro-reconnecting mode frequency, for a given choice of $\bar{k}$ and D, which we take to be real. Our desired solution curves show Λ in the complex plane for a given value of D and several values of $\bar{k}$. Our solutions involve $\bar{k}$ in a range such that D, defined above, can be approximated as independent of $\bar{k}$. We expect the integrals F_0^0 and G_0^0 to introduce an imaginary component to Eq. (3.6) for any nonzero choice of Λ due to the residue from the pole. We define $\Lambda \equiv \Lambda_{Re} + i\gamma$ and separate F_0^0 and G_0^0 into their real and imaginary components so that $F_0^0 = F_{0R}^0 + iF_{0I}^0$ and $G_0^0 = G_{0R}^0 + iG_{0I}^0$. Then we can separate Eq. (3.6) into its real component:

$$\begin{aligned}(\Lambda_{Re}^3 - 3\Lambda_{Re}\gamma^2) + D[(1+F_{0Re}^0)(1-\frac{2(\Lambda_{Re}^2-\gamma^2)}{k^2}) + \frac{4\Lambda_{Re}\gamma}{k^2}F_{0Im}^0]\\ -(\frac{\Lambda_{Re}k^2}{2+2k^2})(1+G_{0Re}^0(1-\frac{2(\Lambda_{Re}^2-\gamma^2)}{k^2}) + G_{0Im}^0\frac{4\Lambda_{Re}\gamma}{k^2})\\ +(\frac{\gamma k^2}{2+2k^2})(G_{0Im}^0(1-\frac{2(\Lambda_{Re}^2-\gamma^2)}{k^2}) - G_{0Re}^0\frac{4\Lambda_{Re}\gamma}{k^2}) = 0\end{aligned} \quad (3.7)$$

And its imaginary component:

$$\begin{aligned}(3\Lambda_{Re}^2\gamma - \gamma^3) + D[(1-\frac{2(\Lambda_{Re}^2-\gamma^2)}{k^2})F_{0Im}^0 - \frac{4\Lambda_{Re}\gamma}{k^2}(1+F_{0Re}^0)]\\ -(\frac{\gamma k^2}{2+2k^2})(1+G_{0Re}^0(1-\frac{2(\Lambda_{Re}^2-\gamma^2)}{k^2}) + G_{0Im}^0\frac{4\Lambda_{Re}\gamma}{k^2})\\ -(\frac{\Lambda_{Re}k^2}{2+2k^2})(G_{0Im}^0(1-\frac{2(\Lambda_{Re}^2-\gamma^2)}{k^2}) - G_{0Re}^0\frac{4\Lambda_{Re}\gamma}{k^2}) = 0\end{aligned} \quad (3.8)$$

To find our desired solution curves, we add the absolute values of the left hand sides of Eq. (3.7) and Eq. (3.8) and search for values of $\bar{k}$, D, and Λ which minimize this

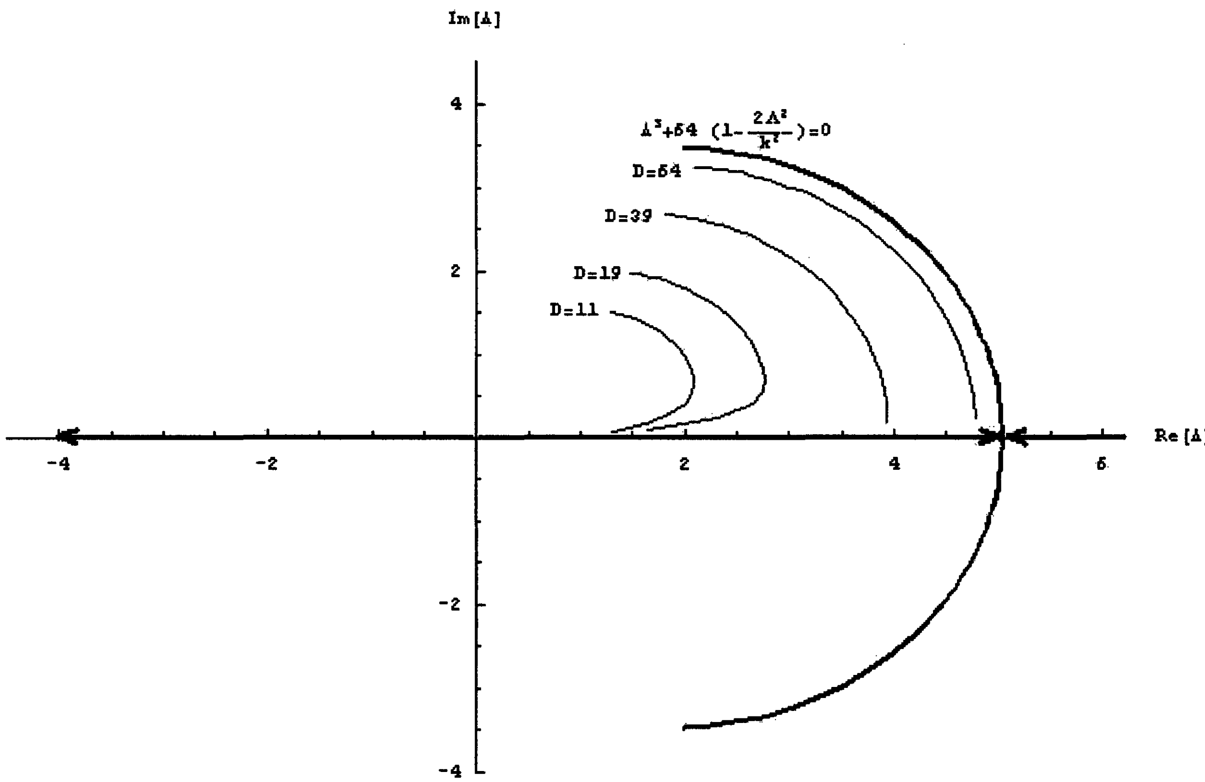

Figure 3.4: Λ in the complex plane for $\bar{k}$ from approximately 3 to 100 and $D = 11, 19, 39, 64$. The bold line shows the solutions of the simplified cubic $\Lambda^3 + D(1 - 2\Lambda^2/\bar{k}^2) = 0$

sum. We find these minima by holding D and Λ_{Re}/γ constant, and sweep over a large range of values of $\bar{k}$ and $|\Lambda|$, looking for the specific combination closest to a zero. Then by succesive iterations of decreasing the sweep range, and increasing the sweep resolution, we find the desired solution point. Then we adjust the ratio Λ_{Re}/γ slightly, and repeat the process for the same value of D. Through this method, we find the solution curves shown in Figure 3.4. We find that for each value of D, as $\bar{k} \to \infty$, Im[Λ]/Re[Λ] approaches some limiting value. Plots of $\bar{k}$ versus Im[Λ]/Re[Λ] are shown in Figure 3.5 for various values of D.

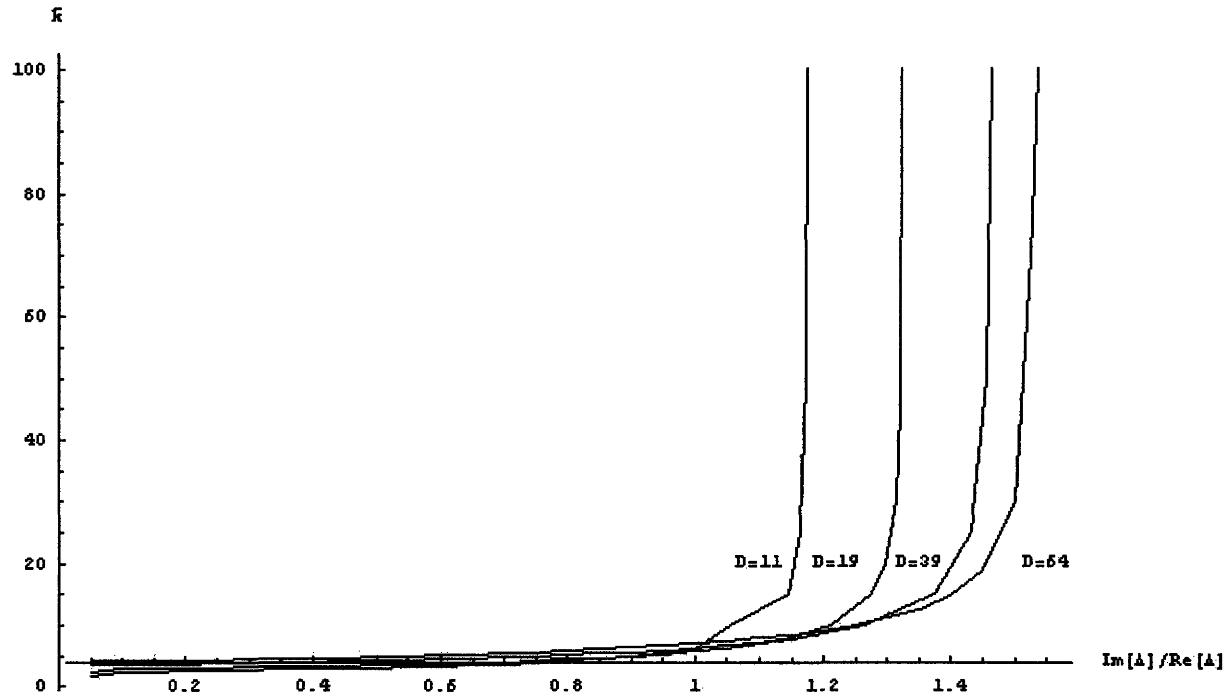

Figure 3.5: Im[Λ]/Re[Λ] for $D = 11, 19, 39, 64$ as $\bar{k} \to \infty$

3.2.1 Theoretical Analysis

We notice in Figure 3.4 that for lower values of D, Λ bends toward the origin as it approaches the real axis. We examine this behavior first by considering the residues of the integrals. In the F_0^0 integral, if you consider the factor of $1/(\Lambda^2 - \xi^2)$, where $\Lambda = \Lambda_{Re} + i\epsilon$, $\epsilon \ll 1$. Then

$$\Lambda^2 - \xi^2 \simeq \Lambda_{Re}^2 + 2i\epsilon\Lambda_{Re} - \xi^2$$

If we define $\Psi \equiv (\Lambda_{Re} - \xi)$, $\Psi \sim \epsilon$, then

$$\xi^2 = \Psi^2 - 2\Lambda_{Re}\Psi + \Lambda_{Re}^2 \simeq \Lambda_{Re}^2 - 2\Lambda_{Re}\Psi$$

and so

$$\Lambda^2 - \xi^2 \simeq \Lambda_{Re}^2 - \xi^2 + 2i\epsilon\Lambda_{Re}$$

$$\simeq \Lambda_{Re}^2 - (\Lambda_{Re}^2 - 2\Lambda_{Re}\Psi) + 2i\epsilon\Lambda_{Re}$$

$$= 2\Lambda_{Re}(i\epsilon + \Psi) = 2\Lambda_{Re}\frac{\epsilon^2 + \Psi^2}{-i\epsilon + \Psi}$$

Thus $1/(\Lambda^2 - \xi^2) \sim (\Psi - i\epsilon)/(2\Lambda_{Re}(\epsilon^2 + \Psi^2))$. Now we take advantage of the fact that the factor of $e^{-\xi^2}$ in the F_0^0 integral sufficiently suppresses the argument of the F_0^0 integral, except when $\xi \rightarrow \Lambda_{Re}$. In that region, the pole will overtake the exponential factor, and we may approximate the value of the entire integral as coming entirely from this region surrounding the pole. Then we may rewrite the integral as such

$$F_0^0 = \frac{1}{\sqrt{\pi}}\int_{-\infty}^{\infty} -d\Psi\, e^{-\Lambda_{Re}^2}(2\Lambda_{Re}^2)\frac{\Lambda_{Re}^2(\Lambda_{Re}^2 - 1/2)}{2\Lambda_{Re}(\epsilon^2 + \Psi^2)}(\Psi - i\epsilon)$$

Where the first negative comes from the $d\xi = -d\Psi$ relation. Considering the imaginary component

$$F_{0Im}^0 \simeq \frac{1}{\sqrt{\pi}}\Lambda_{Re}^5 e^{-\Lambda_{Re}^2}\int_{-\infty}^{\infty} d\Psi\,\frac{1/\epsilon}{1 + \Psi^2/\epsilon^2}$$

Then converting to the variable $\psi \equiv \Psi/\epsilon$ and noting that $d\Psi = \epsilon d\psi$, we find the imaginary residue

$$F_{0Im}^0 \simeq \frac{1}{\sqrt{\pi}}\Lambda_{Re}^5 e^{-\Lambda_{Re}^2}\int_{-\infty}^{\infty} d\psi\,\frac{1}{1 + \psi^2} = \sqrt{\pi}\Lambda_{Re}^5 e^{-\Lambda_{Re}^2} \tag{3.9}$$

The factor of π enters from the arctan integral. Because the real component was of similar magnitude, but opposite sign we say that the real residue goes as $F_{0Re}^0 \simeq -\sqrt{\pi}\Lambda_{Re}^5 e^{-\Lambda_{Re}^2}$. We now wish to examine the behavior of the solutions of Eq. (3.6) when Λ becomes complex. From our result in Eq. (3.9) we see that the terms involving F_0^0 and G_0^0 will always have an imaginary contribution due to the residue, though this contribution is small for Λ_{Re} close to zero, or large. Now we begin with a purely real, first order representation of Eq (3.6)

$$1 + \frac{D}{\Lambda^3}(1 - \frac{2\Lambda^2}{\bar{k}^2}) = 0 \tag{3.10}$$

We then treat the following terms as a complex perturbation

$$F_0^0 + \frac{\bar{k}^2}{(2 + 2\bar{k}^2)\Lambda^2} \tag{3.11}$$

Then if we expand Eq. (3.10) with respect to a solution point Λ_0, we can equate the second order terms to the perturbation above as follows [1]

$$\frac{1}{2}\frac{12\,D}{\Lambda^5}(\delta\Lambda)^2 - \frac{1}{2}\frac{16\,D}{\Lambda^3\,\bar{k}^2}(\delta\Lambda)^2 \simeq F_0^0 + \frac{1}{2\Lambda^2} \tag{3.12}$$

We found a solution near the real axis with $D = 20$, $\bar{k} \simeq 3.1$, $F_0^0 \simeq 1.4 + i\epsilon$, $\epsilon \ll 1$. Plugging these values into our above relation gives us $\delta\Lambda = 1.24 + .175i \rightarrow 8.02°$ for Λ near the real axis. This supports our observed bending of the solutions near the real axis.

Chapter 4

Conclusions

We confirm the driving effect of an electron temperature gradient and the stabilizing effect of a density gradient in these model micro-reconnecting modes. Experiments that can reproduce the conditions of the micro-reconnecting modes can search for these modes with transverse wavelengths of the order of c/ω_{pe}, though the introduction of magnetic shear and the spatial dependence of these modes may alter our theoretical predictions. If these modes are observed, we predict their suppression in the presence of a density gradient.

In future projects we can introduce the effects of magnetic shear, and the spatial dependence of the mode. With this we can get a clearer image of these micro reconnecting modes, and see if the instabilities predicted by the model persist for localized modes. If the instability does persist, as expected, then the resulting microscopic islands may reduce the ratio of parallel to transverse thermal conductivity which would then be capable of producing macroscopic reconnected magnetic surfaces in the plasma as predicted by the micro-reconnecting mode theory. Further analysis of these modes may offer more insight into the present dilemma between drift tearing mode theory and high temperature plasma experimental results.

Chapter 5

Appendix A

We begin with Eq. (2.13)

$$(\omega^3[1+\frac{T_i}{T_e}\frac{\omega_{*e}}{\omega}]+\frac{1}{2}k_\parallel^2c_{se}^2\Omega_*)(d_e^2k_x^2+d_e^2k_y^2)\tilde{A}_\parallel \simeq \omega^2\Omega_*\tilde{A}_\parallel[1+\frac{T_i}{T_e}\frac{\omega_{*e}}{\omega}] \tag{5.1}$$

and the definition of Ω_*.

$$\Omega_* \equiv \frac{\omega^2}{\sqrt{\pi}}\int_{-\infty}^{\infty} du2u^2\mathrm{e}^{-u^2}(\frac{\omega_{*e}+\omega_{*Te}(u^2-1/2)-\omega}{\omega^2-k_\parallel^2v_{te}^2u^2}) \tag{5.2}$$

Now we manipulate our expression for Ω_*.

$$\Omega_* = \frac{\Lambda^2}{\sqrt{\pi}}\int_{-\infty}^{\infty} du2u^2\mathrm{e}^{-u^2}(\frac{\omega_{*e}+\omega_{*Te}(u^2-1/2)-\omega}{\Lambda^2-u^2})$$

where $\Lambda \equiv \omega/|k_\parallel|v_{te}$. Now we separate the different components of the integral Ω_*, and carefully add zero to both components

$$\Omega_* = \omega_{*Te}\frac{\Lambda^2}{\sqrt{\pi}}\int_{-\infty}^{\infty} du2u^2\mathrm{e}^{-u^2}(\frac{(u^2-1/2)-(u^2(u^2-1/2)/\Lambda^2)+(u^2(u^2-1/2)/\Lambda^2)}{\Lambda^2-u^2})$$
$$-(\omega-\omega_{*e})\frac{\Lambda^2}{\sqrt{\pi}}\int_{-\infty}^{\infty} du2u^2\mathrm{e}^{-u^2}(\frac{1-u^2/\Lambda^2+u^2/\Lambda^2}{\Lambda^2-u^2})$$

Now if we carry Λ^2 through the integral, we can change the argument of the integrals as follows

$$\Omega_* = \omega_{*Te}\frac{1}{\sqrt{\pi}}\int_{-\infty}^{\infty} du 2u^2 \mathrm{e}^{-u^2}((u^2-1/2)+\frac{(u^2(u^2-1/2))}{\Lambda^2-u^2})$$
$$-(\omega-\omega_{*e})\frac{1}{\sqrt{\pi}}\int_{-\infty}^{\infty} du 2u^2 \mathrm{e}^{-u^2}(1+\frac{u^2}{\Lambda^2-u^2})$$

We know that $\int_{-\infty}^{\infty}\mathrm{e}^{-u^2}du = \sqrt{\pi}$. Then from integration by parts, we find that $\int_{-\infty}^{\infty}2u^2\mathrm{e}^{-u^2}du = \int_{-\infty}^{\infty}2u^2\mathrm{e}^{-u^2}(u^2-1/2)du = \sqrt{\pi}$. Thus we have

$$\Omega_* = \omega_{*Te} + \omega_{*Te}\frac{1}{\sqrt{\pi}}\int_{-\infty}^{\infty} du 2u^2 \mathrm{e}^{-u^2}(\frac{(u^2(u^2-1/2))}{\Lambda^2-u^2})$$
$$-(\omega-\omega_{*e})-(\omega-\omega_{*e})\frac{1}{\sqrt{\pi}}\int_{-\infty}^{\infty} du 2u^2 \mathrm{e}^{-u^2}(\frac{u^2}{\Lambda^2-u^2})$$

We now define

$$F_0^0 = \frac{1}{\sqrt{\pi}}\int_{-\infty}^{\infty} du 2u^2 \mathrm{e}^{-u^2}(\frac{(u^2(u^2-1/2))}{\Lambda^2-u^2})$$
$$G_0^0 = \frac{1}{\sqrt{\pi}}\int_{-\infty}^{\infty} du 2u^2 \mathrm{e}^{-u^2}(\frac{u^2}{\Lambda^2-u^2})$$

so that

$$\Omega_* = \omega_{*Te}(1+F_0^0)-(\omega-\omega_{*e})(1+G_0^0) \tag{5.3}$$

Refering back to some initial definitions

$$\tau \equiv \frac{T_i}{T_e} \quad \bar{k}^2 \equiv (k_x^2+k_y^2)d_e^2 \quad c_{se}^2 \equiv \tau v_{te}^2$$

we rewrite Eq. (5.3)

$$[\omega^3(1+\tau\frac{\omega_{*e}}{\omega})+\frac{\tau}{2}k_\parallel^2 v_{te}^2(\omega_{*Te}(1+F_0^0))-\frac{\tau}{2}k_\parallel^2 v_{te}^2(\omega-\omega_{*e})(1+G_0^0)](-\bar{k}^2)$$
$$\simeq -\omega^2[1+\tau\frac{\omega_{*e}}{\omega}](\omega_{*Te}(1+F_0^0))+\omega^2[1+\tau\frac{\omega_{*e}}{\omega}](\omega-\omega_{*e})(1+G_0^0)$$

Then dividing through by $|k_\|^3|v_{te}^3$ we find

$$[\Lambda^3(1+\tau\frac{\omega_{*e}}{\omega})+\frac{\tau}{2}\frac{\omega_{*Te}}{|k_\||v_{te}}(1+F_0^0)-\frac{\tau}{2}(\Lambda-\frac{\omega_{*e}}{|k_\||v_{te}})(1+G_0^0)]\bar{k}^2$$
$$\simeq \Lambda^2[1+\tau\frac{\omega_{*e}}{\omega}]\frac{\omega_{*Te}}{|k_\||v_{te}}(1+F_0^0)-\Lambda^2[1+\tau\frac{\omega_{*e}}{\omega}](\Lambda-\frac{\omega_{*e}}{|k_\||v_{te}})(1+G_0^0)$$

Now we introduce the new variables

$$\xi \equiv \frac{\omega_{*Te}}{|k_\||v_{te}} \quad \alpha \equiv \frac{\omega_{*e}}{|k_\||v_{te}}$$

and introduce a factor of $2/\bar{k}^2$ to rewrite our expression as

$$2\Lambda^3(1+\tau\frac{\alpha}{\Lambda})+\tau\xi(1+F_0^0)-\tau(\Lambda-\alpha)(1+G_0^0)$$
$$\simeq \frac{2\Lambda^2}{\bar{k}^2}[1+\tau\frac{\alpha}{\Lambda}]\xi(1+F_0^0)-\frac{2\Lambda^2}{\bar{k}^2}[1+\tau\frac{\alpha}{\Lambda}](\Lambda-\alpha)(1+G_0^0)$$

Rearranging yields

$$\Lambda^3(\frac{2+2\bar{k}^2}{\bar{k}^2})+\xi\tau[1-\frac{2\Lambda^2}{\bar{k}^2\tau}](1+F_0^0)-\alpha\xi\tau\frac{2\Lambda}{\bar{k}^2}(1+F_0^0)+2\alpha\Lambda^2\tau$$
$$\simeq [\tau\Lambda+(\tau\Lambda-\frac{2\Lambda^3}{\bar{k}^2})G_0^0]-\alpha[\tau-\frac{2\Lambda^2}{\bar{k}^2}(1-\tau)-\frac{2\Lambda}{\bar{k}^2}\alpha\tau](1+G_0^0)$$

Defining $D=\xi\tau\bar{k}^2/(2+2\bar{k}^2)$ we arrive at

$$\Lambda^3+D[1-\frac{2\Lambda^2}{\bar{k}^2\tau}](1+F_0^0)-\alpha D\frac{2\Lambda}{\bar{k}^2}(1+F_0^0)+\alpha\Lambda^2\tau\frac{\bar{k}^2}{1+\bar{k}^2}$$
$$\simeq \frac{\bar{k}^2}{2+2\bar{k}^2}[\Lambda\tau+(\Lambda\tau-\frac{2\Lambda^3}{\bar{k}^2})G_0^0]-\alpha\frac{\bar{k}^2}{2+2\bar{k}^2}[\tau-\frac{2\Lambda^2}{\bar{k}^2}(1-\tau)-\frac{2\Lambda}{\bar{k}^2}\alpha\tau](1+G_0^0) \quad (5.4)$$

Bibliography

[1] B. Coppi. Unpublished notes on the micro-reconnecting plasma mode dispersion relation derivation.

[2] B. Coppi. Theoretical resolution of magnetic reconnection in high energy plasmas. In *Collective Phenomena in Macroscopic Systems*, pg. 59, Publ. World Scientific, 2007.

[3] U. S. DOE. U.s. climate change technology program. *Strategic Plan*, pages 82–83, 2006.

[4] J. A. Snipes, R. S. Granetz, R. J. Hastie, A. E. Hubbard, Y. In, D. Mossessian, J. E. Rice, J. J. Ramos, D. Schmittdiel, G. Taylor, and S. M. Wolfe. β limiting mhd activity and mode locking in alcator c-mod. In *Plasma Physics and Controlled Fusion*, Institute of Physics Publishing, 44:381-393, 2002.